

Study of $J/\psi \rightarrow p\bar{p}\phi$

LIU Qian, YUAN Changzheng

Using 58 M J/ψ events collected at BESII, the up limit on the branching fraction for cascade decay $J/\psi \rightarrow p\bar{p}f_0, f_0 \rightarrow \pi^+\pi^-$ is measured to be 9×10^{-5} at 90% confidence level and that for $J/\psi \rightarrow p\bar{p}f_0, f_0 \rightarrow K_S^0 K_S^0$ is 7×10^{-6} . The branching fraction of $J/\psi \rightarrow p\bar{p}\phi$ is measured as $Br_{J/\psi \rightarrow p\bar{p}\phi} = (5.17 \pm 1.70_{stat.} \pm 0.68_{sys.}) \times 10^{-5}$, where the first error is statistical and the second is systematic.

PACS numbers:

I. INTRODUCTION

In recent two years, a near-threshold enhancement in the $p\bar{p}$ invariant mass spectrum was observed from $B^+ \rightarrow K^+ p\bar{p}$ and $\bar{B}^0 \rightarrow D^0 p\bar{p}$ by Belle [1][2], and then BESII reported a similar phenomena in the $J/\psi \rightarrow \gamma p\bar{p}$ [3]. This enhancement can be fitted with an S-wave Breit-Wigner resonance function with a mass about 1.860 GeV and a width less than 30 MeV at 90% C.L. Lots of theories try to explain it, such as the final state interaction [4], multi-quark and so on. And for our experiment, we are searching for the $p\bar{p}$ enhancement in the other $p\bar{p}V$ decay modes, such as: $J/\psi \rightarrow p\bar{p}\omega$ [5], $J/\psi \rightarrow p\bar{p}\rho$ [6], but no enhancement is observed. Here, we try to look for the $p\bar{p}$ enhancement in $J/\psi \rightarrow p\bar{p}\phi$.

In pp collisions, some experiments are searching for the cryptoexotic baryons with hidden strangeness, such as $B_\phi = udds\bar{s}$ [7]. It is expected that these penta-quark baryons have a narrow width and decay preferentially into the ϕN , $K\bar{K}N$ and so on. They have observed a narrow peak in the $\Sigma(1385)^0 K^+$ spectra, and believe that this should be able to be observed in the $p\phi$ spectra. So we will also try to look for this B_ϕ state in $J/\psi \rightarrow p\bar{p}\phi$.

Since in $J/\psi \rightarrow p\bar{p}\phi$ decay mode, the phase space is very small, if we try to measure this channel by $\phi \rightarrow K^+ K^-$ mode, the phase space will be smaller, the momentum of K is so small that lots of K will decay to μ . So here we'll try to do this analysis through $J/\psi \rightarrow p\bar{p}\phi, \phi \rightarrow K_S^0 K_L^0$ mode.

II. BES DETECTOR

The upgraded BESII is located at the Beijing Electron-Positron Collider (BEPC) in the Institute of High Energy Physics in Beijing. BESII is a large solid-angle magnetic spectrometer which is described in detail in [8]. The momentum of the charged particle is determined by a 40-layer cylindrical main drift chamber (MDC) which has a momentum resolution of $\sigma_p/p = 1.78\% \sqrt{1 + p^2(\text{GeV}^2)}$. Particle identification is accomplished by specific ionization (dE/dx) measurements in the drift chamber and time-of-flight (TOF) information in a barrel-like array of 48 scintillation counters. The dE/dx resolution is $\sigma_{dE/dx} = 8.0\%$; the TOF resolution for Bhabha events is $\sigma_{TOF} = 180\text{ps}$. Radially outside of the time-of-flight counters is a 12-radiation-length barrel shower counter (BSC) comprised of gas proportional tubes interleaved with lead sheets. The BSC measures the energy and direction of photons with resolutions of $\sigma_E/E \approx 21\%/\sqrt{E(\text{GeV})}$, $\sigma_\phi = 7.9\text{mrad}$, and $\sigma_z = 2.3\text{cm}$. Outside of the solenoidal coil, which provides a 0.4 Tesla magnetic field over the tracking volume, is an iron flux return that is instrumented with three double layers of counters that identify muons of momentum greater than $0.5\text{ GeV}/c$. It provides coordinate measurements along the muon trajectories with resolutions in the outermost layer of 10 cm and 12 cm in r_ϕ and z . The solid angle coverage of the layers is 67%, 67% and 63% of 4π , respectively.

A GEANT3 based Monte Carlo package (SIMBES) with detailed consideration of the detector performance is used. The consistency between data and Monte Carlo simulation has been carefully checked in many high purity physics channels, and the agreement is reasonable. The detection efficiency and mass resolution for each decay modes are obtained from Monte Carlo simulation which takes into account the angular distributions in different final states.

III. PROTON PARTICLE IDENTIFICATION (PID) EFFICIENCY

Since in this analysis, the momentum of p and \bar{p} are less than 0.6 GeV. Generally speaking, when the particle's momentum is less than 1.0 GeV, the energy deposit combined with the momentum allows excellent particle identification. Ref. [9] shows

the energy deposit versus the momentum for each kinds of particles. However, when the proton is "slow", the deposited energy might be too large to be measured by ADC. And since most of the "slow" proton's energy are deposited in the MDC detector, it's difficult for "slow" p to hit the TOF detector, but for \bar{p} , lots of sub-particles are generated from \bar{p} reacting with the material of MDC, the TOF information is still available.

To do the PID, we define:

$$X_i = \frac{(dE/dx)_{Measurement} - (dE/dx)_{expectation}}{\sigma_{dE/dx}}.$$

and

$$T_i = \frac{(TOF)_{Measurement} - (TOF)_{expectation}}{\sigma_{TOF}}$$

here dE/dx is the energy deposit per unit length, and σ is the resolution, i for different particle hypothesis, ($i = \pi, K, p$). From the definition, X_i and T_i should be normal standard distribution. Usually, the X_i and T_i are combined to calculate χ_i^2 for each particle hypothesis, and relatively weight criteria: $\chi_p^2 < \chi_K^2$, $\chi_p^2 < \chi_\pi^2$ is used as the proton PID. Fig. 1 shows the efficiency of p and \bar{p} PID using this criteria, the difference between data and MC simulation is larger in the low momentum region of p , while since the difference is small for \bar{p} , we'll use this criteria for \bar{p} PID.

The "slow" p sample is selected from $J/\psi \rightarrow p\bar{p}\pi^+\pi^-$. An event is required to have 4 charged tracks, and the total charge must be 0, each of which is well fitted to a helix within the polar angle region $|\cos\theta| < 0.8$ and with the point of closest approach of the track to the beam line within the interaction region of $\sqrt{x_0^2 + y_0^2} < 2$ cm, $|z_0| < 20$ cm. The transverse momentum of each track is required to be greater than 70 MeV/c, which is the minimum needed to reach the outer radius of the BSC in the 0.4 Tesla magnetic field.

Two pions are required to be identified by dE/dx and TOF information. When dealing with the p PID efficiency, \bar{p} is required to be identified, and vice versa. To remove the backgrounds containing γ , such as $J/\psi \rightarrow \Sigma^0\bar{\Sigma}^0$, the invariant mass of these 4 tracks, M_{tot} , is required to satisfy: $|M_{tot} - M_{J/\psi}| < 0.06$ GeV. To remove the backgrounds containing π^0 , the U_{miss} must be satisfied with: $|U_{miss}| < 0.1$ GeV.

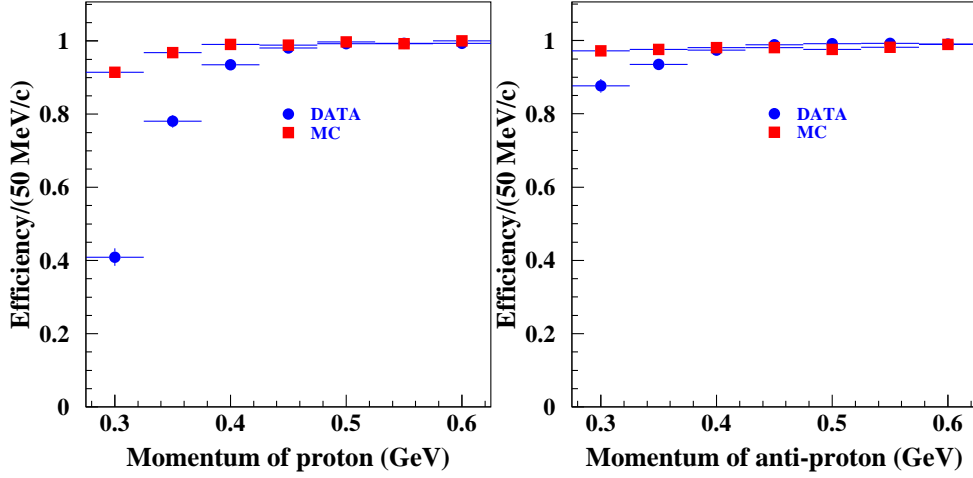


FIG. 1: p and \bar{p} PID efficiency using $\chi_{sp}^2 < \chi_{sK}^2, \chi_{sp}^2 < \chi_{s\pi}^2$.

To remove $J/\psi \rightarrow \Lambda\bar{\Lambda}$, the invariant mass of p and π , $M_{p\pi^-,\bar{p}\pi^+}$, is required as $|M_{p\pi^-,\bar{p}\pi^+} - M_\Lambda| > 0.01$ GeV. To remove $J/\psi \rightarrow \Delta^{++}\bar{\Delta}^{--}$, $M_{p\pi^+,\bar{p}\pi^-} > 1.35$ GeV is required. Also, 4C kinematic fit for $p\bar{p}\pi^+\pi^-$ is performed and the probability is required to be greater than 0.01.

Here we only focus on the p and \bar{p} the momentum of which are less than 0.6 GeV. From J/ψ data, the number of the selected p and \bar{p} sample is 5496 and 5010 respectively. For Monte-Carlo simulation, 1×10^5 events are generated using HOWL generator (FLUKA mode), and about 4250 and 4086 events are selected as the MC simulated p and \bar{p} sample respectively. The reason why p sample is larger than \bar{p} is that the PID efficiency of p is less than \bar{p} .

Fig. 2 shows the X_π, X_K and X_p distribution of p and \bar{p} at different momentum region determined from data. A long tail of X_p exists at the low momentum proton's X_p distribution, and the behaviour of p and \bar{p} is similar. Fig. 3 shows the Monte-Carlo simulation result. According to this, the PID of p is required as:

$$\begin{cases} X_p < 2, X_K > 2 & p_p < 0.425 \text{ GeV} \\ \chi_p^2 < \chi_K^2, \chi_p^2 < \chi_\pi^2 & p_p > 0.425 \text{ GeV} \end{cases} \quad (1)$$

Fig. 4 shows the efficiency of p and \bar{p} PID using the new criteria, the difference

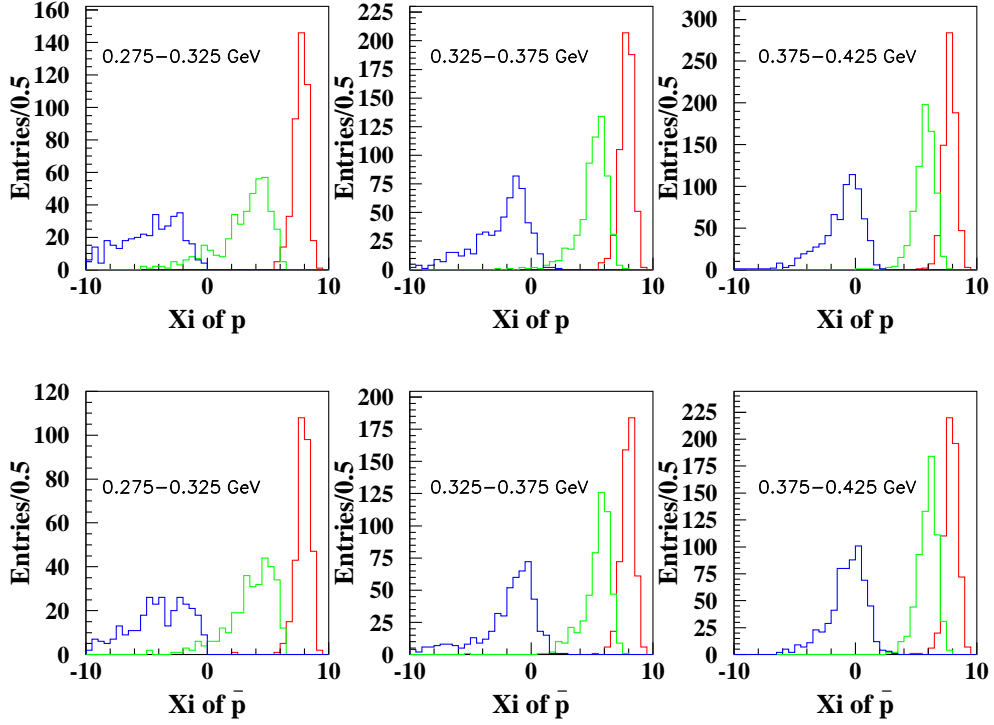


FIG. 2: The X_π, X_K and X_p of p and \bar{p} in different momentum region determined from data. The blue one is X_p , the green one is X_K , and the red one is X_π .

between data and MC simulation is smaller now except for the first bin.

IV. ANALYSIS OF $J/\psi \rightarrow p\bar{p}f_0(980), f_0(980) \rightarrow K_S^0 K_S^0$

Through the study of J/ψ 30 M Monte-Carlo simulated inclusive data, $J/\psi \rightarrow p\bar{p}f_0(980), f_0(980) \rightarrow K_S^0 K_S^0$ is shown as the main background of our signal channel $J/\psi \rightarrow p\bar{p}\phi, \phi \rightarrow K_S^0 K_L^0$. Since $f_0(980)$ decaying into $\pi^+\pi^-$ is dominated, so we try to measure the branching fraction of $J/\psi \rightarrow p\bar{p}f_0(980), f_0(980) \rightarrow K_S^0 K_S^0$ through $J/\psi \rightarrow p\bar{p}f_0(980), f_0(980) \rightarrow \pi^+\pi^-$.

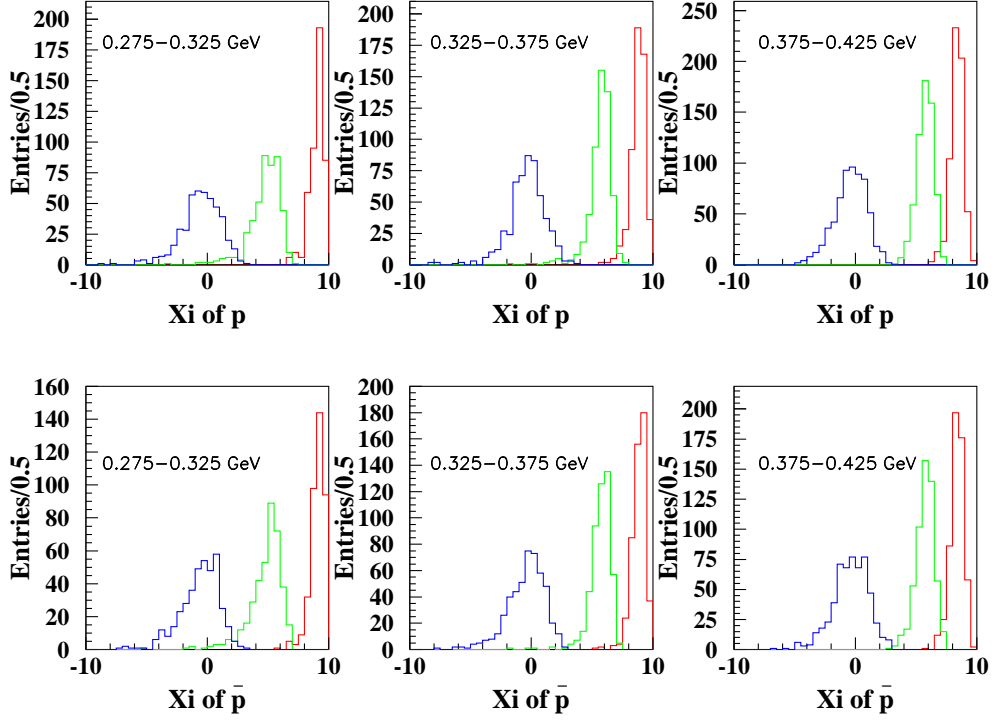


FIG. 3: The X_π, X_K and X_p of p and \bar{p} in different momentum region determined from Monte-Carlo. The blue one is X_p , the green one is X_K , and the red one is X_π .

A. Event selection for $J/\psi \rightarrow p\bar{p}f_0(980), f_0(980) \rightarrow \pi^+\pi^-$

An event is required to have 4 charged tracks with good helix fit, $|\cos\theta| < 0.8$, and $\sqrt{x_0^2 + y_0^2} < 2$ cm, $|z_0| < 20$ cm. The total charge of these 4 tracks must 0. p, \bar{p}, π^+, π^- are all required to be identified by dE/dx and TOF information. For p and \bar{p} PID, Eq. 1 is used, and for π^+ and π^- , $\chi_{s\pi}^2 < \chi_{sK}^2, \chi_{s\pi}^2 < \chi_{sp}^2$ is required. And then the probability of 4C kinematic fit is required to be greater than 0.01.

To remove the Λ signal, $|M_{p\pi^-, \bar{p}\pi^+} - M_\Lambda| > 0.0075$ GeV is required. Fig 5 shows the $M_{p\pi^-}$ distribution, a clear Λ signal can be seen. Fig 6 shows the fit result of Λ signal, the resolution is about 0.0024 GeV.

To remove the Δ signal, $M_{p\pi^+, \bar{p}\pi^-} > 1.35$ GeV is required. Fig 7 shows the $M_{p\pi^+}$ distribution, and Fig 8 shows the fit result of Δ signal. The red arrow shows the cut.

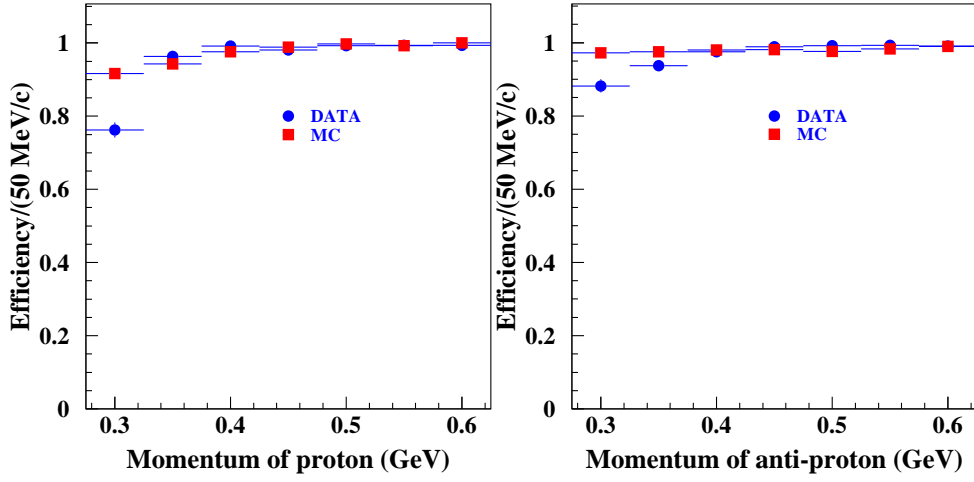


FIG. 4: p PID efficiency using the new criteria.

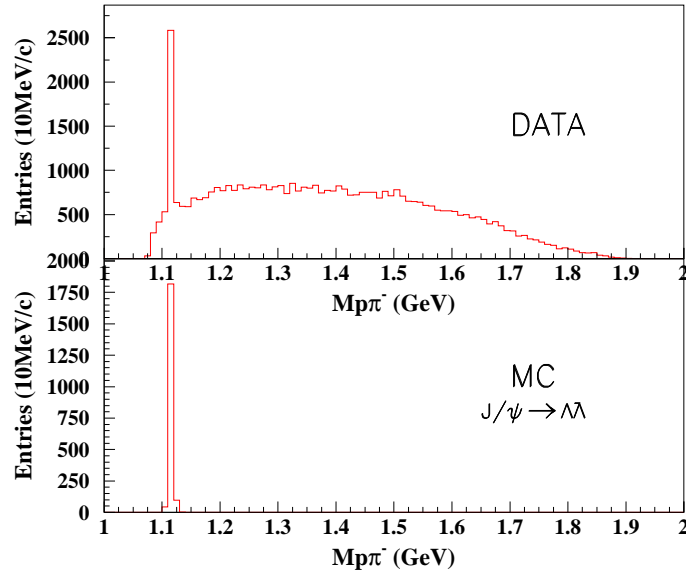


FIG. 5: $M_{p\pi^-}$ distribution of data and Monte-Carlo.

After these selections, Fig 9 shows the detection efficiency, reconstructed $m_{\pi^+\pi^-}$ offset and resolution vary with the $m_{\pi^+\pi^-}$ which is gotten from Monte-Carlo simulation. At each point of $m_{\pi^+\pi^-}$ mass, 1×10^5 events are generated. The mass offset is 2 MeV less than the input value. The resolution increases a little, this is because

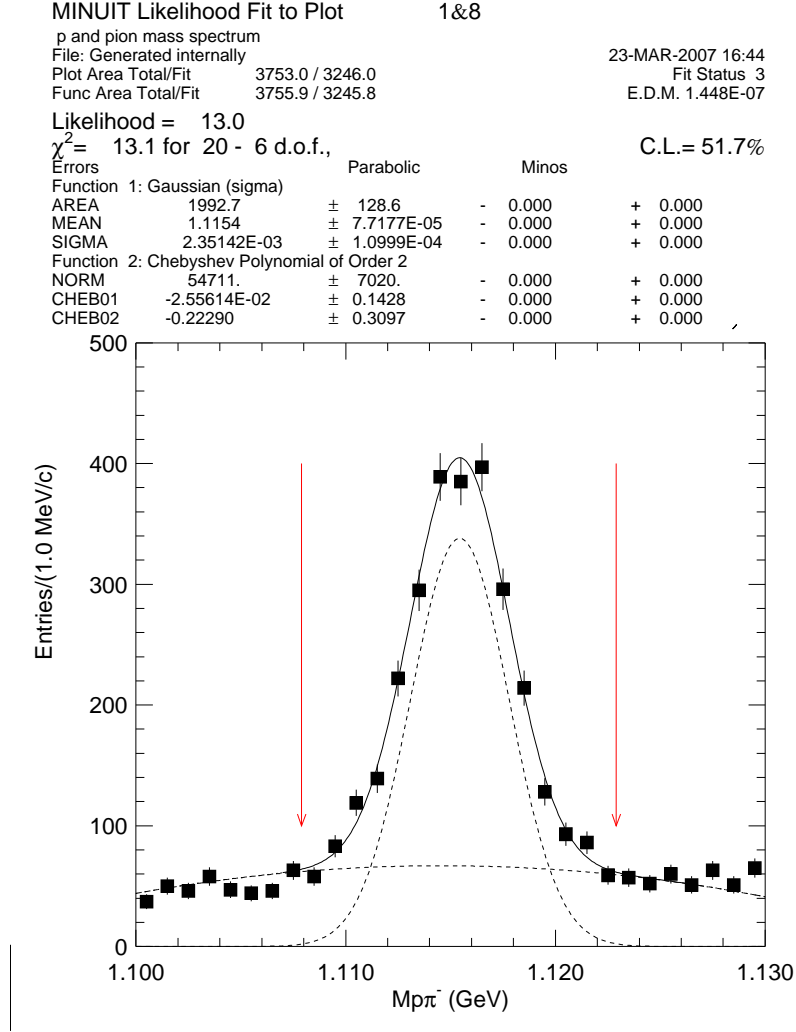


FIG. 6: Fit the Λ signal. The red arrows show the cut.

of the low momentum particles' detection resolution.

B. Fit formula

The $f_0(980)$ is fitted with the usual Flatté formula:

$$f = \frac{1}{M^2 - s - i(g_1\rho_{\pi\pi} + g_2\rho_{K\bar{K}})}$$

where $\rho_{\pi\pi, K\bar{K}}$ are the phase space factor for $\pi\pi$ and $K\bar{K}$ channels, and $g_{1,2}$ are squares of coupling constants to these two channels, s is the center-mass energy, m_K is taken as the average for K^0 and K^\pm . The Table I gives the numbers and

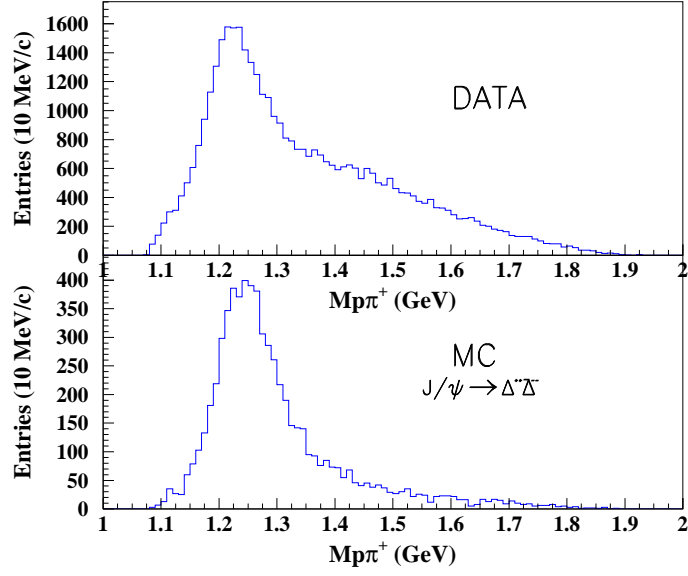


FIG. 7: $M_{p\pi^+}$ distribution of data and Monte-Carlo.

equations [10]:

TABLE I: The number of $g_{1,2}$ and $\rho_{\pi\pi, K\bar{K}}$

$$\begin{aligned}
 M &= 965 \pm 10 \text{ MeV} \\
 g_1 &= 165 \pm 18 \text{ MeV} \\
 g_2 &= 695 \pm 92 \text{ MeV} \\
 \rho_{\pi\pi} &= \sqrt{1 - \frac{4m_\pi^2}{s}} \\
 \rho_{K\bar{K}} &= \begin{cases} 0 & s < 4m_K^2 \\ \sqrt{1 - \frac{4m_K^2}{s}} & s \geq 4m_K^2 \end{cases}
 \end{aligned}$$

If the mass of $f_0(980)$ is larger than the $K\bar{K}$ threshold, it's very easy to decay through $K\bar{K}$ channel, so the width of $f_0(980)$ is asymmetric. The number of $f_0(980) \rightarrow \pi^+\pi^-$ or $K_S^0 K_S^0$ events can be calculated by:

MINUIT Likelihood Fit to Plot 1&8
 PHYANALY. kspcc axis
 File: Generated internally 23-MAR-2007 22:23
 Plot Area Total/Fit 41934. / 41934. Fit Status 3
 Func Area Total/Fit 40676. / 41934. E.D.M. 1.600E-06

Likelihood = 845.3
 $\chi^2 = 864.7$ for 38 - 5 d.o.f., C.L.= 0.00 %

Errors	Parabolic	Minos		
Function 1: Histogram 1 7 Normal errors				
NORM 2.6592	$\pm 4.7250E-02$	- 0.000	+ 0.000	
Function 2: Chebyshev Polynomial of Order 3				
NORM 16949.	± 218.7	- 0.000	+ 0.000	
CHEB01 0.47845	$\pm 1.5082E-02$	- 0.000	+ 0.000	
CHEB02 -1.9802	$\pm 2.6225E-02$	- 0.000	+ 0.000	
CHEB03 0.86764	$\pm 2.5718E-02$	- 0.000	+ 0.000	

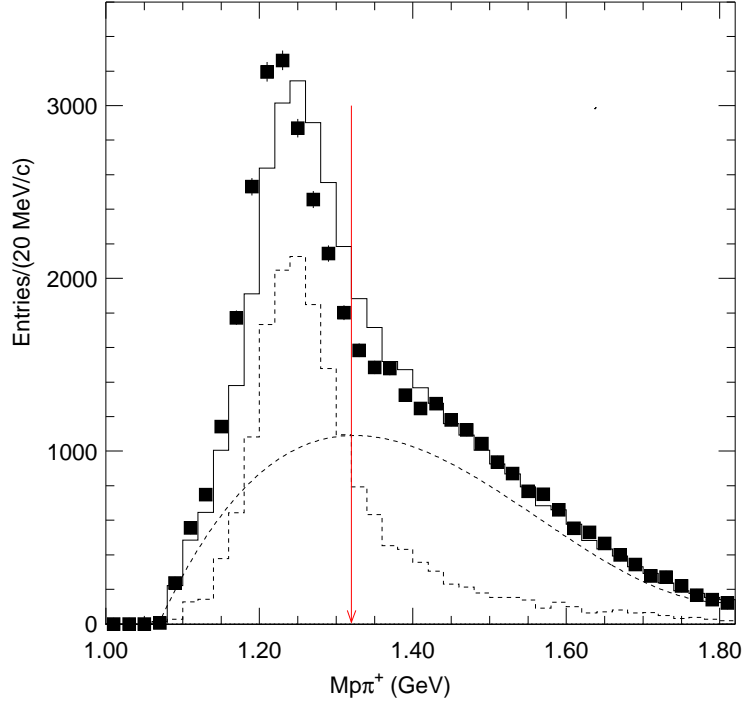


FIG. 8: Fit the Δ signal. The red arrow shows the cut.

$$\begin{aligned}
 N_{f_0 \rightarrow \pi^+ \pi^-} &= \frac{2}{3} \int_{0.9}^{1.2} ds |f(980)|^2 \rho_{\pi\pi} \\
 N_{f_0 \rightarrow K_S^0 K_S^0} &= \frac{1}{4} \int_{1.0}^{1.2} ds |f(980)|^2 \rho_{K\bar{K}}
 \end{aligned} \tag{2}$$

The factors take into account the facts that: two-thirds of $\pi\pi$ decays into $\pi^+\pi^-$ and one third of $\pi^0\pi^0$, and half of $K\bar{K}$ decays into K^+K^- and half to $K^0\bar{K}^0$, and half of $K^0\bar{K}^0$ decays into $K_S^0 K_S^0$ and half to $K_L^0 K_L^0$. The fitted $f_0(980) \rightarrow \pi^+\pi^-$ signal is integrated over the mass range from 0.9 to 1.2 GeV and $K_S^0 K_S^0$ is from 1.0 to 1.2 GeV [10].

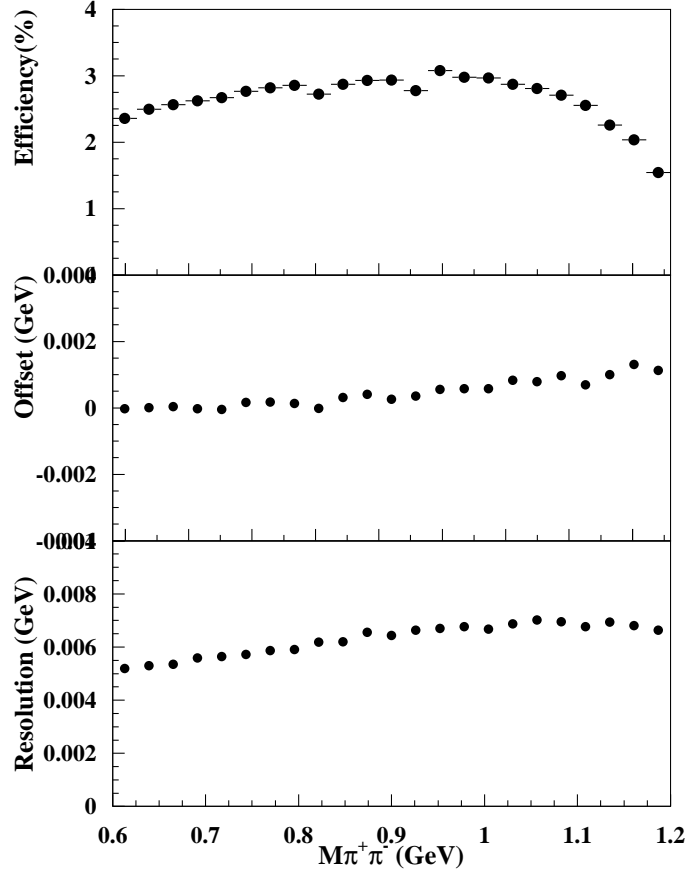


FIG. 9: The selection efficiency, $m_{\pi^+\pi^-}$ mass offset and resolution vary with the $\pi^+\pi^-$ invariant mass.

When fitting the $N_{f_0 \rightarrow \pi^+\pi^-}$, the fit function can be written as:

$$\frac{dN_{f_0 \rightarrow \pi^+\pi^-}}{dm_{\pi^+\pi^-}} \propto \frac{2}{3} \cdot \frac{d(\int ds |f(980)|^2 \rho_{\pi\pi})}{dm_{\pi^+\pi^-}}$$

where $s = (m_{\pi^+\pi^-})^2$, then we can get:

$$\begin{aligned} \frac{dN_{f_0 \rightarrow \pi^+\pi^-}}{dm_{\pi^+\pi^-}} &\propto \frac{2}{3} \cdot 2m_{\pi^+\pi^-} \cdot |f(980)|^2 \rho_{\pi\pi} \\ &\propto \frac{2}{3} \cdot 2m_{\pi^+\pi^-} \cdot \frac{1}{(M^2 - (m_{\pi^+\pi^-})^2)^2 + M^2(g_1\rho_{\pi\pi} + g_2\rho_{K\bar{K}})^2} \cdot \rho_{\pi\pi} \end{aligned}$$

So the final fit function $f(m_{\pi^+\pi^-})$ can be written as:

$$f(m_{\pi^+\pi^-}) = c \cdot \frac{dN_{f_0 \rightarrow \pi^+\pi^-}}{dm_{\pi^+\pi^-}}$$

where c is the fitted parameter. So the $N_{f_0 \rightarrow \pi^+\pi^-}$ can be calculated by:

$$N_{f_0 \rightarrow \pi^+\pi^-} = \int f(m_{\pi^+\pi^-}) \cdot dm_{\pi^+\pi^-} \quad (3)$$

To take into account the selection efficiency, $\varepsilon(m_{\pi^+\pi^-})$, which is shown in Fig 9, the combined function f' would be:

$$f' = f(m_{\pi^+\pi^-}) \cdot \varepsilon(m_{\pi^+\pi^-})$$

C. The $f_0(980)$ signal

Fig. 10 shows the $m_{\pi^+\pi^-}$ distribution. Since the $f_0(980)$ signal is very small, the Bayes method is employed to calculate the upper limit of this channel, and we got $c = 400$ for 90% confidence level. Using Eq. 3, the number of f_0 signal is $N_{f_0 \rightarrow \pi^+\pi^-} = 4583.9$.

D. Systematic Error

1. Proton Tracking

The proton tracking efficiency is also studied through $J/\psi \rightarrow p\bar{p}\pi^+\pi^-$. Fig. 11 shows the p and \bar{p} tracking efficiency of data and Monte-Carlo simulation in different momentum region. The systematic error for p and \bar{p} tracking is estimated as $\sum_i (\sigma_{\varepsilon_i} / \varepsilon_i) \omega_i$, where ε_i is the p and \bar{p} tracking efficiency in the i -th momentum bin determined from data, σ_{ε_i} is the error of ε_i , and ω_i is the fraction of MC simulated $J/\psi \rightarrow p\bar{p}f_0(980), f_0(980) \rightarrow \pi^+\pi^-$ events in the same bin at generator level. Table II shows the numbers. 5.5% and 3.4% are taken as the systematic error for p and \bar{p} tracking, respectively.

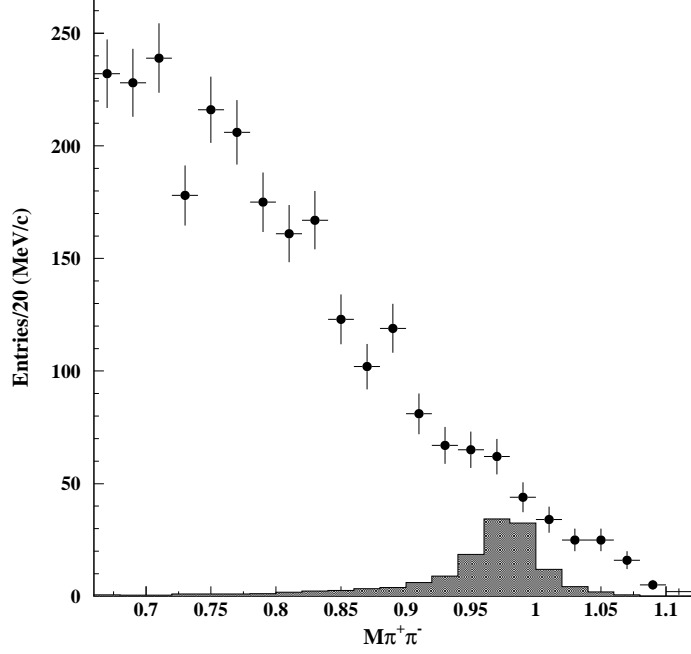


FIG. 10: The distribution of $m_{\pi^+\pi^-}$, the dot is data, the histogram is the Monte-Carlo simulated which is not normalized.

2. Particle Identification

The systematic error for π PID is studied by $J/\psi \rightarrow \rho\pi$ sample, and 1% is taken as the systematic error for each π track.

Same as the proton tracking, the systematic error for p PID is calculated as $\sum_i (\sigma_{\varepsilon'_i} / \varepsilon'_i) \omega_i$, where ε'_i is the proton PID efficiency and has been shown in Fig. 4. Table III shows the numbers, 3.8% and 2.6% are taken as the systematic error for p and \bar{p} PID, respectively.

3. Kinematic fit

$J/\psi \rightarrow \Lambda\bar{\Lambda}$ is chosen to study the systematic error of 4C kinematic fit. This sample is selected through: 4 good MDC tracks and the other common criteria. The track whose momentum is larger than 0.7 GeV is assumed to be a proton, and

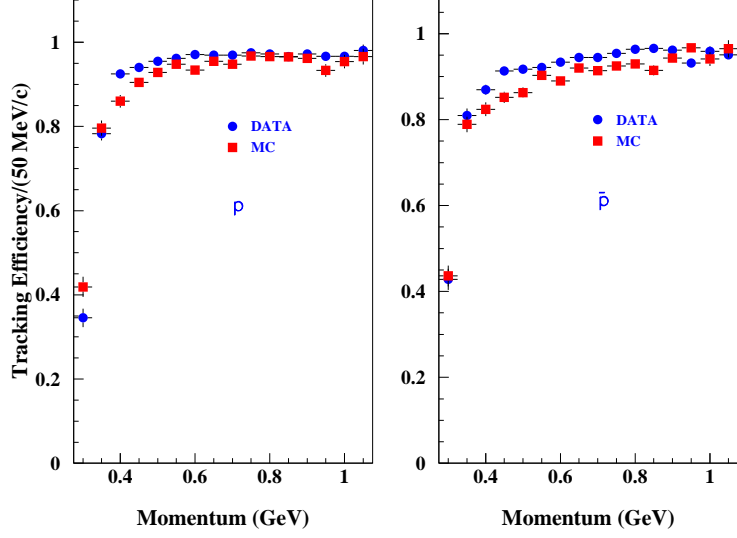


FIG. 11: The p and \bar{p} tracking efficiency versus the momentum of proton.

TABLE II: The ω_i , ε_i of p and \bar{p} in the different momentum region.

Region (GeV)	ω_i (%)	ε_i^p (%)	$\varepsilon_i^{\bar{p}}$ (%)
0.275 – 0.325	14.8	34.5 ± 7.4	42.8 ± 0.8
0.325 – 0.375	17.2	78.3 ± 1.3	80.9 ± 2.0
0.375 – 0.425	17.5	92.5 ± 6.5	86.9 ± 4.5
0.425 – 0.475	17.4	94.0 ± 3.5	91.3 ± 6.1
0.475 – 0.525	7.8	95.5 ± 2.7	91.7 ± 5.4
0.525 – 0.575	5.5	96.2 ± 1.4	92.2 ± 1.9

the track whose momentum is less than 0.32 GeV is assumed to be a pion. The invariant mass of p and π should be satisfied with: $|m_{p\pi^-, \bar{p}\pi^+} - m_\Lambda| < 0.0075$ GeV and the decay length of Λ should be larger than 5 mm. To remove the $J/\psi \rightarrow \Sigma^0 \bar{\Sigma}^0$ background, the invariant mass of Λ and $\bar{\Lambda}$ should be greater than 3.03 GeV.

The 4C kinematic fit efficiencies for data and Monte-Carlo simulation are 87.97% and 90.79% (call ptrk function), 3.21% is taken as the systematic error for 4C

TABLE III: The ω_i , ε_i^p of p and \bar{p} in the different momentum region.

Region (GeV)	$\omega_i(\%)$	$\varepsilon_i^p(\%)$	$\varepsilon_i^{\bar{p}}(\%)$
0.275 – 0.325	14.8	76.2 ± 15.4	88.2 ± 9.0
0.325 – 0.375	17.2	96.3 ± 2.1	93.7 ± 3.9
0.375 – 0.425	17.5	99.1 ± 1.5	97.5 ± 0.6
0.425 – 0.475	17.4	98.0 ± 0.8	98.9 ± 0.8
0.475 – 0.525	7.8	99.2 ± 0.5	99.2 ± 1.6
0.525 – 0.575	5.5	99.3 ± 0.1	99.3 ± 0.9

kinematic fit.

4. Mass cut

To remove the Λ signal, $|M_{p\pi^-, \bar{p}\pi^+} - M_\Lambda| > 0.0075$ GeV is required. It's a very narrow mass window. When we change the mass window from 0.0075 GeV (3σ) to 0.01 GeV (4σ), the number of observed events doesn't change, the systematic error for this cut is neglected.

To remove the Δ signal, $M_{p\pi^+, \bar{p}\pi^-} > 1.35$ GeV is required. The systematic error for this cut comes from two parts:

- Mass resolution difference between data and Monte-Carlo simulation.

From the K_S^0 and Λ mass resolution of data and Monte-Carlo simulation, we can draw a conclusion that the difference of mass resolution between data and Monte-Carlo simulation is small and can be neglected.

- Different typologies.

Let's assume that there are two more typologies which can decays into $p\bar{p}f_0(980)$: $J/\psi \rightarrow pX$, $X \rightarrow \bar{p}f_0(980)$ and $J/\psi \rightarrow Xf_0(980)$, $X \rightarrow p\bar{p}$. Table IV shows the

efficiency of $M_{p\pi^+, \bar{p}\pi^-} > 1.35$ GeV for different typologies and different mass of X . The biggest difference would be 8.7%, and it is taken as the systematic error for this mass cut.

TABLE IV: The mass cut efficiency for different typologies and different mass of X .

typology	m_X (GeV)	efficiency (%)
$J/\psi \rightarrow p\bar{p}f_0$	–	62.9
$J/\psi \rightarrow pX, X \rightarrow \bar{p}f_0$	1.95	64.5
$J/\psi \rightarrow pX, X \rightarrow \bar{p}f_0$	2.1	61.0
$J/\psi \rightarrow Xf_0, X \rightarrow p\bar{p}$	1.9	61.1
$J/\psi \rightarrow Xf_0, X \rightarrow p\bar{p}$	2.1	68.4

5. Total systematic error

Table V shows the summary of systematic errors. The total systematic error is 13.3%.

E. Branching fraction calculation

Substitute the numbers given in Table I into Eq. 2, we can get:

$$\frac{N_{f_0 \rightarrow K_S^0 K_S^0}}{N_{f_0 \rightarrow \pi^+ \pi^-}} = \frac{\frac{1}{4} \int_{1.0}^{1.2} ds |f(980)|^2 \rho_{K\bar{K}}}{\frac{2}{3} \int_{0.9}^{1.2} ds |f(980)|^2 \rho_{\pi\pi}} = 0.077$$

and we've gotten:

$$N_{f_0 \rightarrow \pi^+ \pi^-} = 4583.9 \quad (CL = 90\%)$$

so

TABLE V: Summary of systematic errors

<i>source</i>	σ_{sys}
π tracking	4.0%
p tracking	5.5%
\bar{p} tracking	3.4%
π PID	2.0%
p PID	3.8%
\bar{p} PID	2.6%
4C fit	3.2%
remove Λ	neglect
remove Δ	8.7%
$N_{J/\psi}$	4.7%
<i>Tot</i>	13.3%

$$N_{f_0 \rightarrow K_S^0 K_S^0} = 353.0 \quad (CL = 90\%)$$

The upper limter of branching fraction of $J/\psi \rightarrow p\bar{p}f_0(980)$, $f_0(980) \rightarrow K_S^0 K_S^0$ is:

$$Br_{(J/\psi \rightarrow p\bar{p}f_0, f_0 \rightarrow K_S^0 K_S^0)} = \frac{N_{f_0 \rightarrow K_S^0 K_S^0}}{N_{J/\psi} \cdot (1 - \sigma_{sys})} \leq 7 \times 10^{-6} \quad (CL = 90\%)$$

and

$$Br_{(J/\psi \rightarrow p\bar{p}f_0, f_0 \rightarrow \pi^+ \pi^-)} = \frac{N_{f_0 \rightarrow \pi^+ \pi^-}}{N_{J/\psi} \cdot (1 - \sigma_{sys})} \leq 9 \times 10^{-5} \quad (CL = 90\%)$$

Since this branching fraction is very small, it can be neglected.

V. ANALYSIS OF $J/\psi \rightarrow p\bar{p}\phi, \phi \rightarrow K_S^0 K_L^0$

A. Event selection

An event is required to have 4 charged tracks with good helix fit, $|\cos\theta| < 0.8$, and the total charge of these 4 tracks must 0. p, \bar{p} are required to be identified by dE/dx and TOF information. And then one K_S^0 must be reconstructed, the decay length of K_S^0 must be greater than 5 mm. Fig. 12 shows the fit result of K_S^0 distribution determined from data, the resolution, $\sigma_{K_S^0}$, is about 5 MeV. So we require that $\left| M_{\pi^+\pi^-} - M_{K_S^0} \right| < 15$ MeV.

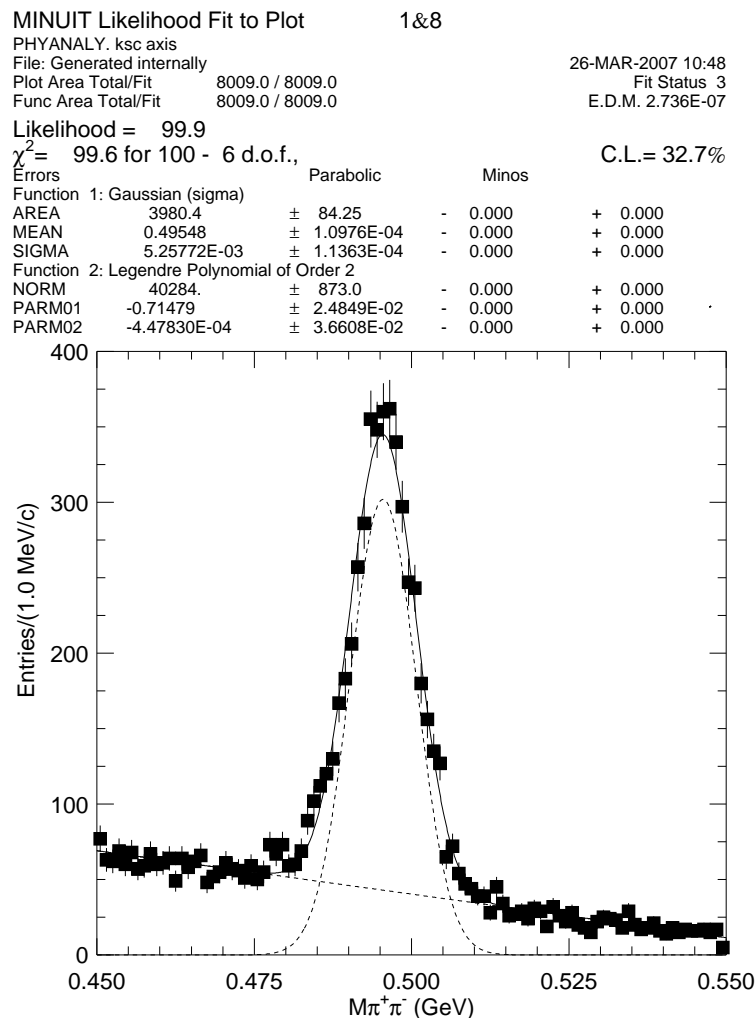


FIG. 12: The distribution of $m_{\pi^+\pi^-}$.

Fig. 13 shows the missing mass distribution. The first one is determined from data, and the shaded histogram is got from K_S^0 sideband which is: $\left| M_{\pi^+\pi^-} - (M_{K_S^0} \pm 5 \cdot \sigma_{K_S^0}) \right| < 1.5 \cdot \sigma_{K_S^0}$; a clear π^0 signal can be seen and it mainly comes from $J/\psi \rightarrow \bar{p}K_S^0\Sigma^+ + c.c., \Sigma^+ \rightarrow p\pi^0$. The enhancement around the 0.3 GeV maybe come from $J/\psi \rightarrow \bar{p}K^*\Sigma^+ + c.c., K^* \rightarrow K_S^0\pi^0$ cascade decay.

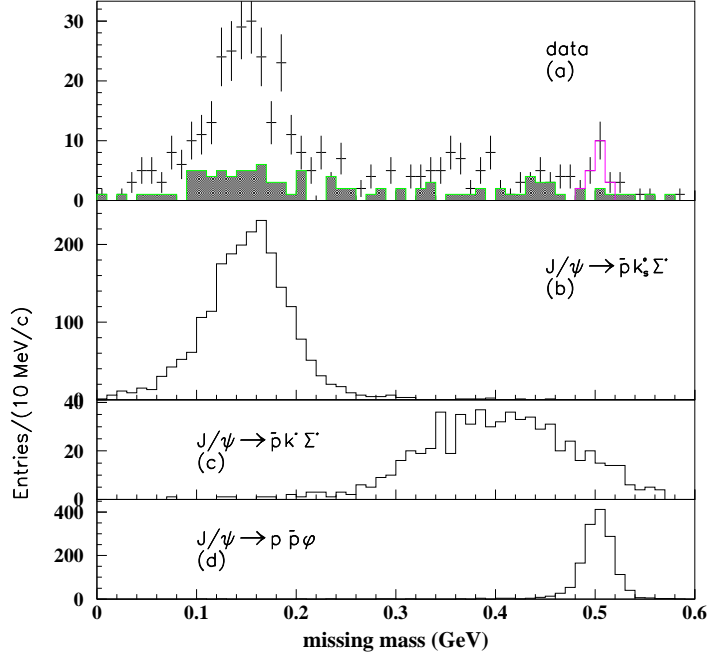
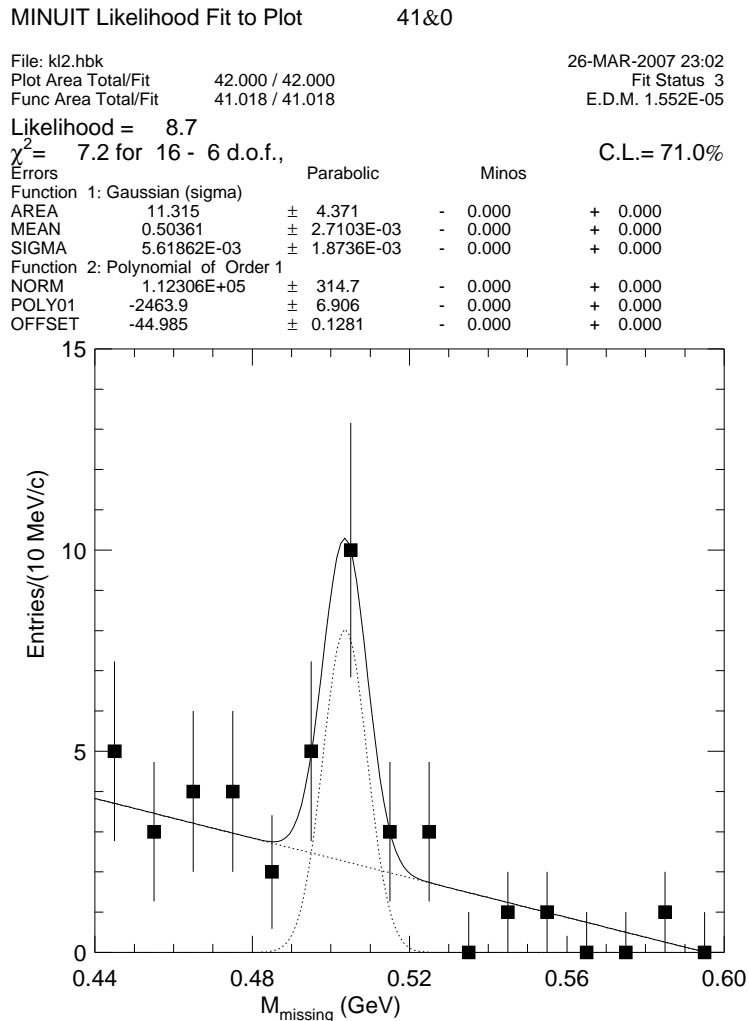


FIG. 13: The missing mass distribution. (a) is determined from data, (b) (c) (d) are MC simulated $J/\psi \rightarrow \bar{p}K_S^0\Sigma^+$, $J/\psi \rightarrow \bar{p}K^*\Sigma^+$, $J/\psi \rightarrow p\bar{p}\phi$, respectively.

Fig. 14 shows the fitted K_L^0 signal result, the resolution is about 6 MeV. $\left| M_{\pi^+\pi^-} - M_{K_L^0} \right| < 0.02$ GeV is required and the pink histogram in Fig. 13 (a) shows the selected region

Then we employ the 1C kinematic fit and require the probability of 1C kinematic fit to be greater than 0.01. Fig. 15 gives the result. Since 1C kinematic fit does not show any improvement to the signal, we will not use this criteria.

FIG. 14: The fitted K_L^0 result.

B. Backgrounds and ϕ signal

Possible backgrounds are simulated using HOWL generator. Table VI shows the result, where N_{norm} is the normalized N_{norm} according to the branching fraction respectively. Except for the $J/\psi \rightarrow p\bar{p}f_0, f_0 \rightarrow K_S^0 K_S^0$, the other backgrounds have little contributions. Fig. 16 shows the $m_{K_S^0 K_L^0}$ versus the missing mass. Since there is no $K_L^0 \pi^+ \pi^-$ background due to the S conservation, only 4 regions are selected as the 2-D sideband region shown as the boxes. Fig. 17 shows the ϕ signal and the shaded histogram is the background distribution which is gotten from the 2-D sideband. Fig. 18 shows the Monte-Carlo simulated ϕ signal. The width of ϕ signal

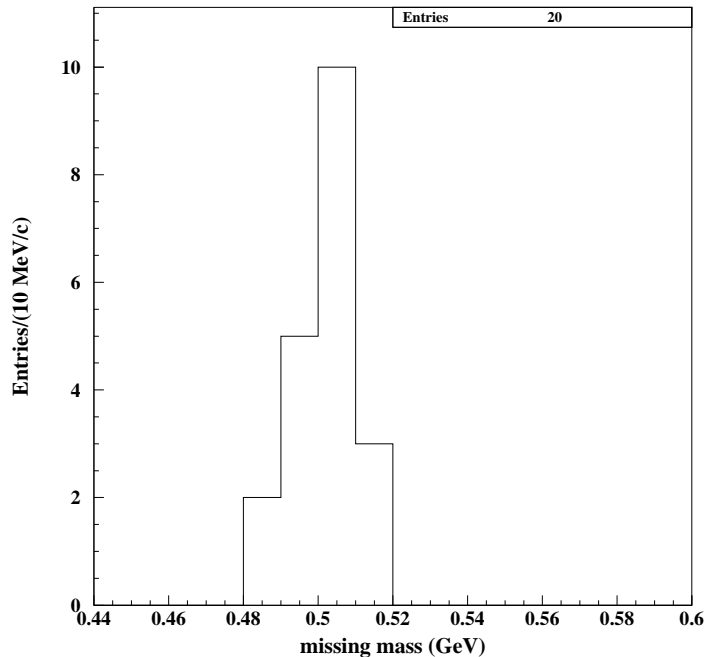


FIG. 15: The missing mass distribution after 1C kinematic fit.

of Monte-Carlo simulated is consistent with data.

The number of observed events, N_{obs} , is 20.0 ± 4.5 , the number of background, N_{bg} , is 5.3 ± 1.1 , and the detection efficiency, ε , is 1.35% (Since in the Monte-Carlo simulation we didn't point out the K_S^0 decay mode, so the detection efficiency has included the branching fraction of $K_S^0 \rightarrow \pi^+\pi^-$). The branching fraction of $J/\psi \rightarrow p\bar{p}\phi$ is calculated as:

$$\begin{aligned} Br_{J/\psi \rightarrow p\bar{p}\phi} &= \frac{N_{obs} - N_{bg}}{\varepsilon \times N_{J/\psi} \times Br(\phi \rightarrow K_S^0 K_L^0)} \\ &= (5.17 \pm 1.70_{stat.}) \times 10^{-5} \end{aligned}$$

In order to deal with the dependence between the detection efficiency and $K_S^0 K_L^0$ invariant mass, the mass bin-by-bin detection efficiency correction is also done. Fig. 19 shows the detection efficiency versus the $K_S^0 K_L^0$ invariant mass. For each mass point, 1×10^5 events are generated. The branching fraction of $J/\psi \rightarrow p\bar{p}\phi$ is calculated by:

TABLE VI: Summary of the Monte-Carlo simulated backgrounds

$J/\psi \rightarrow channel$	N_{theory}	N_{gen}	N_{obs}	N_{norm}
$J/\psi \rightarrow \gamma K^+ K^- \pi^+ \pi^-$	120960	2×10^5	0	0
$J/\psi \rightarrow \gamma p \bar{p} \pi^+ \pi^-$	45504	5×10^4	0	0
$J/\psi \rightarrow p \bar{p} \pi^+ \pi^- \pi^0$	132480	2×10^5	0	0
$J/\psi \rightarrow p \bar{p} \omega, \omega \rightarrow \pi^+ \pi^- \pi^0$	44561	2×10^5	0	0
$J/\psi \rightarrow p \bar{p} \eta', \eta' \rightarrow \pi^+ \pi^- \eta, \eta \rightarrow \gamma \gamma$	9118	1×10^4	0	0
$J/\psi \rightarrow p \bar{p} \eta', \eta' \rightarrow \pi^+ \pi^- \eta, \eta \rightarrow 3\pi^0$	7517	1×10^4	0	0
$J/\psi \rightarrow p \bar{p} \eta', \eta' \rightarrow \pi^0 \pi^0 \eta, \eta \rightarrow \pi^+ \pi^- \pi^0$	2465	1×10^4	0	0
$J/\psi \rightarrow p \bar{p} \phi, \phi \rightarrow K^+ K^-$	1273	1×10^4	0	0
$J/\psi \rightarrow p K^{*-} \bar{\Lambda}, K^{*-} \rightarrow K_S \pi^-, \bar{\Lambda} \rightarrow \bar{p} \pi^+$	–	1×10^5	0	0
$J/\psi \rightarrow \gamma K^+ K^- K_S K_L$	–	5×10^4	0	0
$J/\psi \rightarrow \gamma \phi \phi, \phi \rightarrow K_S K_L$	2663	5×10^4	0	0
$J/\psi \rightarrow \gamma \phi_1 \phi_2, \phi_1 \rightarrow K_S K_L, \phi_2 \rightarrow K^+ K^-$	3854	5×10^4	0	0
$J/\psi \rightarrow p \bar{p} f_0(980), f_0(980) \rightarrow K_S K_S$	–	1×10^5	1530	–

$$Br_{J/\psi \rightarrow p \bar{p} \phi} = \frac{\sum_i \frac{(N_{obs}^i - N_{bg}^i)}{\varepsilon_i}}{N_{J/\psi} \times Br(\phi \rightarrow K_S^0 K_L^0)}$$

where N_{obs}^i is the number of ϕ event shown in Fig. 17 blank histogram in each bin, N_{bg}^i is the number of 2-D sideband shown in Fig. 17 shaded histogram in the same bin, ε_i is the detection efficiency shown in Fig. 19 in the same bin. The branching fraction is:

$$Br_{J/\psi \rightarrow p \bar{p} \phi} = (5.48 \pm 1.72_{stat.}) \times 10^{-5}$$

These two results are consistent in errors, and we choose the first method to calculated the branching fraction.

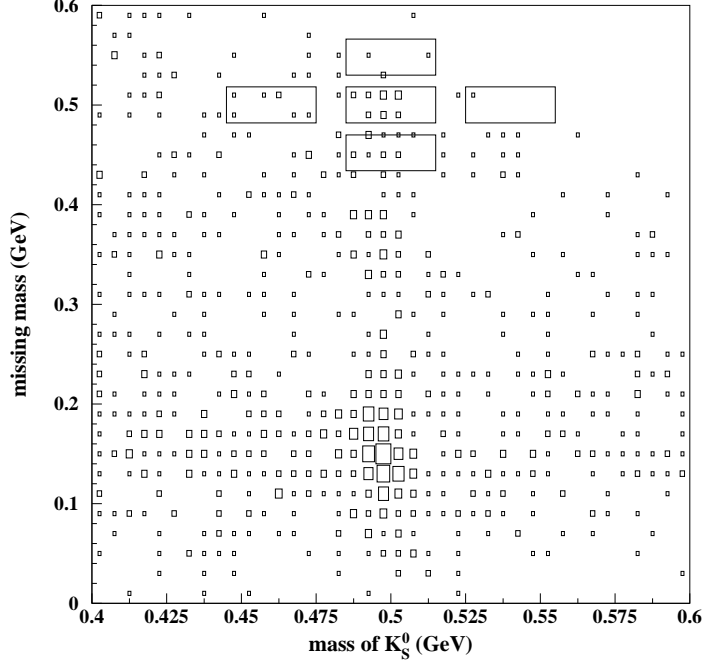


FIG. 16: The $m_{K_S^0 K_L^0}$ versus the missing mass distribution, the boxes show the signal region and 2-D sideband region.

C. The data quality check

1. Detection efficiency, mass offset and resolution

Fig. 19 shows the detection efficiency versus the $K_S^0 K_L^0$ invariant mass, reconstructed $m_{K_S^0 K_L^0}$ offset and resolution vary with the $K_S^0 K_L^0$ invariant mass. The detection efficiency becomes smaller when $m_{K_S^0 K_L^0}$ increases, this is mainly because the detection efficiency for lower momentum p and \bar{p} (< 0.2 GeV) is nearly zero.

2. Cross Check

From Fig. 13, a clear π^0 signal can be seen and it mainly comes from $J/\psi \rightarrow \bar{p}K_S^0 \Sigma^+ + c.c., \Sigma^+ \rightarrow p\pi^0$. The branching fraction of this channel is estimated as: $Br_{J/\psi \rightarrow pK_S^0 \bar{\Sigma}^-} = (3.1 \pm 0.4_{stat.}) \times 10^{-4}$ where the error is only statistical, and the

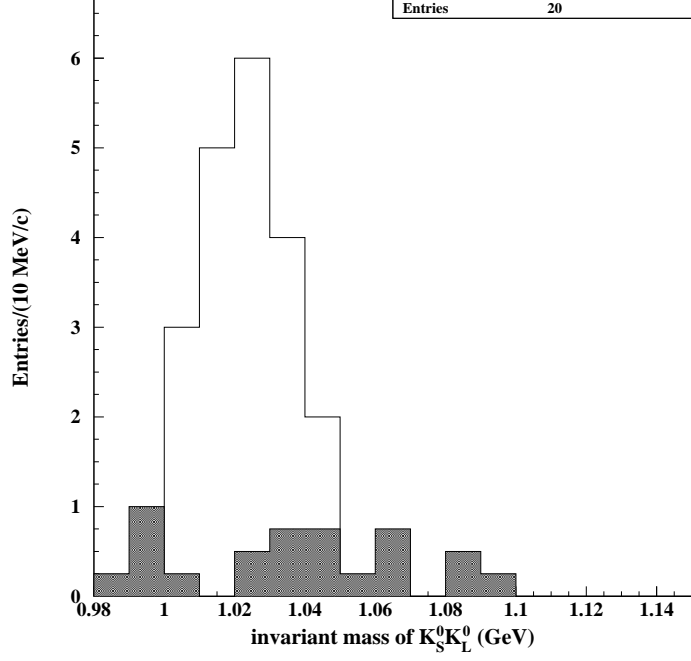


FIG. 17: The $m_{K_S^0 K_L^0}$ distribution, the shaded histogram is the background which is gotten from 2-D sideband.

result is consistent in errors with the Ref. [11].

D. Systematic Error

1. proton tracking and PID

Similar to the $J/\psi \rightarrow p\bar{p}f_0(980)$, the systematic error for tracking is 5.4% and 3.6% for p and \bar{p} , respectively; the systematic error for PID is 3.6% and 2.5% for p and \bar{p} , respectively.

2. K_S^0 reconstruction

The K_S^0 sample is selected from $J/\psi \rightarrow K^{*\pm}K^\mp; K^{*\pm} \rightarrow K_S^0\pi^\pm$ [12]. Fig 20 shows the K_S^0 reconstruction efficiency versus the momentum of K_S^0 . The average of

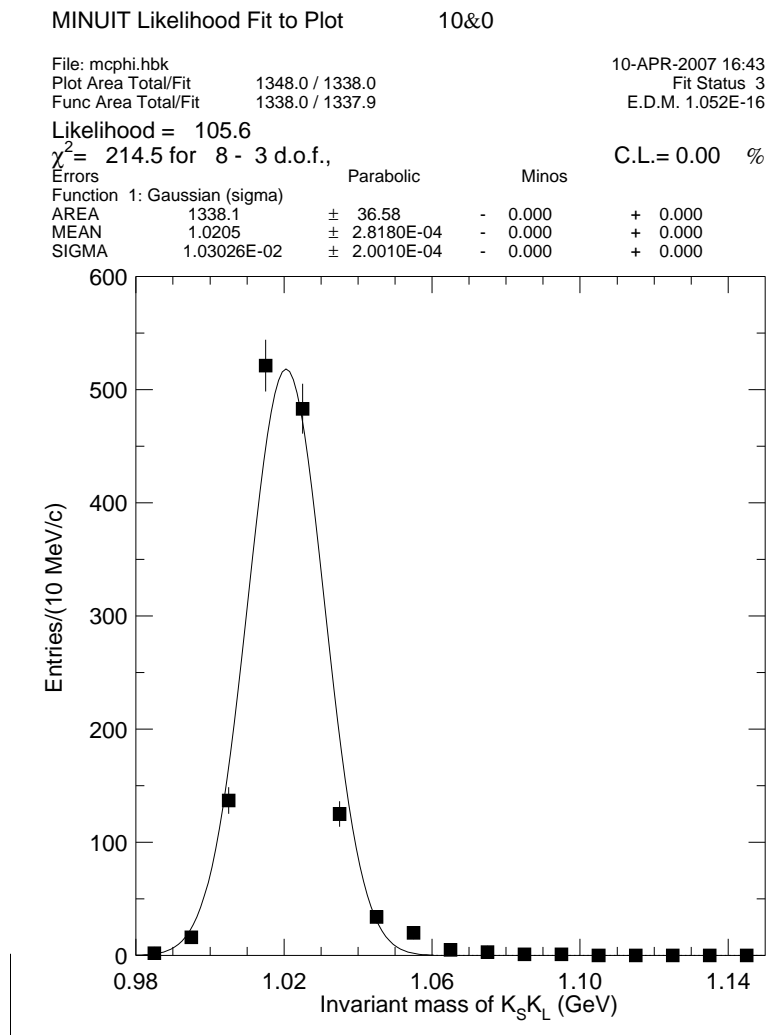


FIG. 18: The fit result of Monte-Carlo simulated ϕ signal.

$\varepsilon_{data}^{K_S^0} / \varepsilon_{MC}^{K_S^0} = 97.6\%$, so the systematic error for K_S^0 reconstruction is taken as 2.4%.

3. Total systematic error

Table VII shows the summary of systematic errors. The total systematic error is 13.2%, so the branching fraction is $Br_{J/\psi \rightarrow p\bar{p}\phi} = (5.17 \pm 1.70_{stat.} \pm 0.68_{sys.}) \times 10^{-5}$.

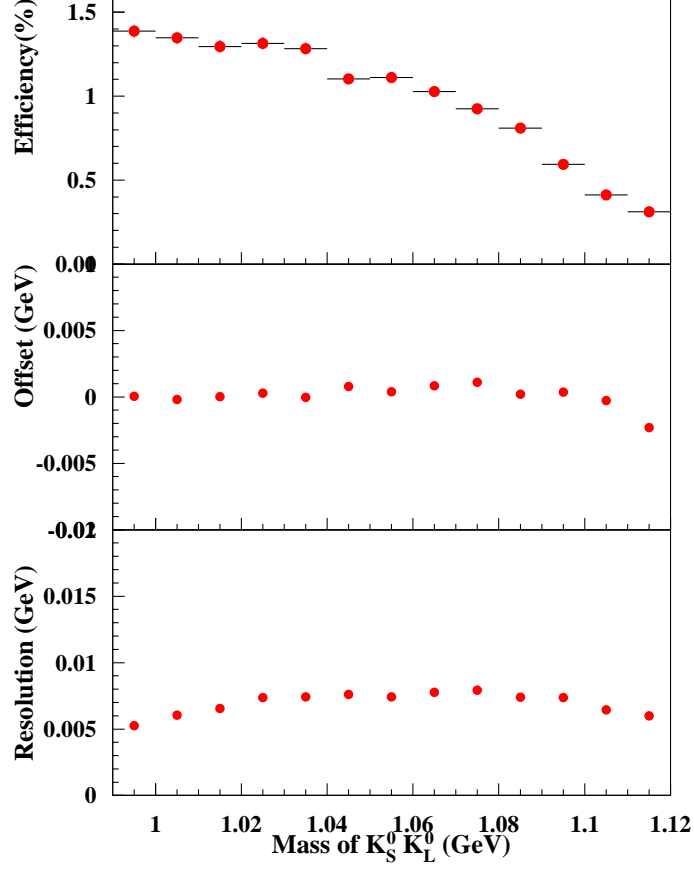


FIG. 19: The selection efficiency, reconstructed $m_{K_S^0 K_L^0}$ offset and resolution vary with the $K_S^0 K_L^0$ invariant mass.

E. Discussion

Fig. 21 gives the $m_{p\bar{p}}$ distribution after requiring $|m_{K_S^0 K_L^0} - m_\phi| < 20$ MeV, (a) the dots with error bar is determined from data, the shaded histogram is the 2-D sideband background, (b) the blank histogram is the Monte-Carlo simulated phase space process: $J/\psi \rightarrow p\bar{p}K_S^0 K_L^0$. Fig. 22 shows the invariant mass of p and ϕ of data. Since the low statistic, no evidence for $p\bar{p}$ and $p\bar{\phi}$ enhancement observed.

:7/03/26 23.03

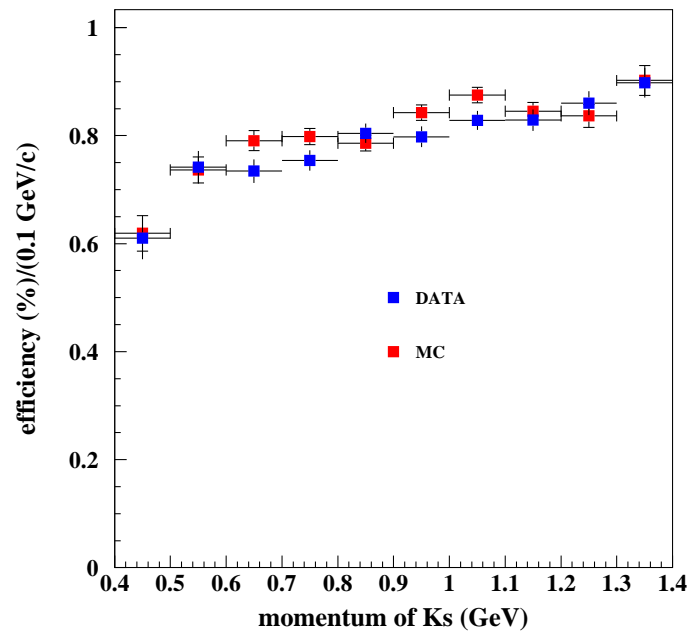


FIG. 20: The K_S^0 reconstruction efficiency versus the momentum of K_S^0 .

-
- [1] K. Abe *et al.*, Phys. Rev. Lett. **88**, 181803 (2002).
 - [2] K. Abe *et al.*, Phys. Rev. Lett. **89**, 151802 (2002).
 - [3] J. Z. Bai *et al.*, Phys. Rev. Lett. **91**, 022001 (2003).
 - [4] J. Haidenbauer *et al.*, Phys. Rev. **D74**, 017501 (2006).
 - [5] B. J. LIU *et al.*, Study of J/ψ decays into $\omega p \bar{p}$, BES memo.
 - [6] B. X. Zhang. *et al.*, BES memo.
 - [7] A. Sibirtsev *et al.* nucl-th0512055.
 - [8] J. Z. Bai *et al.*, Nucl. Instr. Meth. A **458**,627(2001).
 - [9] W.-M. Yao *et al.*, J. Phys. G **33**, 1(2006)
 - [10] J. Z. Bai *et al.*, Phys.Lett. **B607** (2005) 243-253
 - [11] Study of $J/\psi \rightarrow p K^- \bar{\Sigma}^0 + c.c.$ & $J/\psi \rightarrow p K_S^0 \bar{\Sigma}^- + c.c.$ BES memo.
 - [12] Z. WANG *et al.*, HEP&NP, 27, 1 (2003)

TABLE VII: Summary of systematic errors

<i>source</i>	σ_{sys}
π tracking	4.0%
p tracking	5.4%
\bar{p} tracking	3.5%
π PID	2.0%
p PID	3.6%
\bar{p} PID	2.5%
K_S^0 reconstruction	2.4%
N_{bg}	8.0%
$N_{J/\psi}$	4.7%
$Br(\phi \rightarrow K_S^0 K_L^0)$	1.5%
$Br(K_S^0 \rightarrow \pi^+ \pi^-)$	0.2%
<i>Tot</i>	13.2%

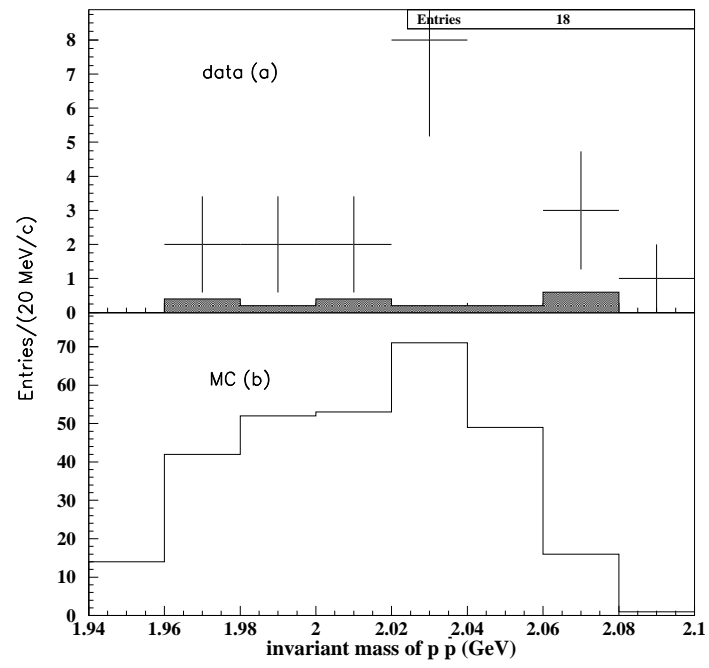
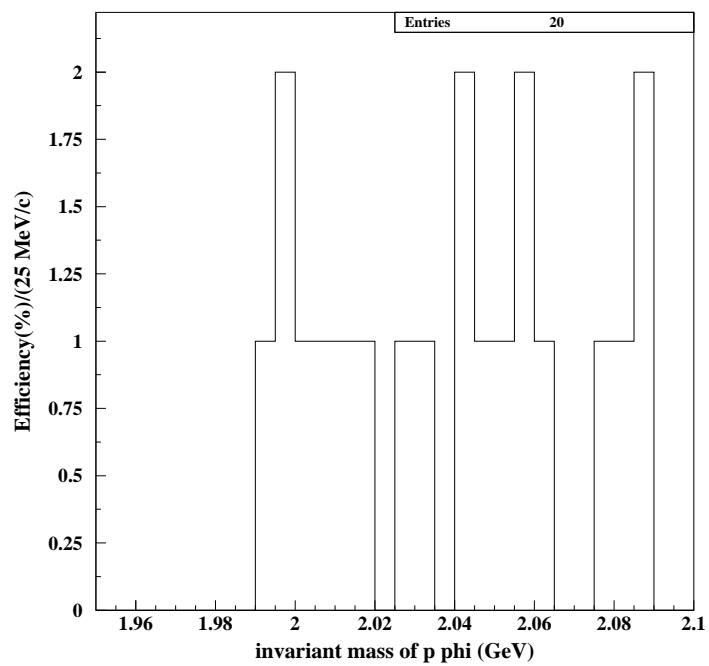


FIG. 21: The $m_{p\bar{p}}$ distribution, the meaning of each histogram is described in the text.

FIG. 22: The invariant mass of p and ϕ .